Numerical analysis of strongly coupled multicore photonic crystal fibres for multiplexer and de-multiplexer applications

Journal of Physics: Conference Series **2322** (2022) 012077 doi:10.1088/1742-6596/2322/1/012077

Numerical analysis of strongly coupled multicore photonic crystal fibres for multiplexer and de-multiplexer applications

M Mohammed[1], **A K Ahmad**[2]
[1]Department of Physics, College of Science, Mustansiriyah University, Baghdad, Iraq
[1]Institute of Applied Physics, University of Muenster, Correnstr.2-4, 48149 Muenster, Germany
[2]Department of Physics, College of Science, AL-Nahrain University, Baghdad, Iraq
Email:[1]dr.miamiph@uomustansiriyah.edu.iq

Abstract. In this study, the coupling properties of multicore photonic crystal fibers (MCPCFs) are analyzed numerically using COMSOL Multiphysics 5.5, based on the finite element method. The dependence of the coupling properties on the structure of the MCPCFs and the wavelength are investigated to realize applications such as multiplexers-demultiplexers for wavelength division multiplexing. The effective mode indexes and transverse electric field distributions of multiple cores are evaluated for different spatial configurations of identical and non-identical cores. A slight change in the central core diameter relative to adjacent cores leads to non-identical cores that lead to wavelength-dependent coupling properties, such as the coupling lengths and strength of the coefficients. The results show that the coupling lengths become longer and the strength coefficients become smaller as the wavelength decreases for non-identical cores than the identical cores. The introduction of anisotropy to all core diameters shows that the coupling lengths become longer and the strength of the coefficients become smaller as the wavelength decreases as well, and both values become lower than the ones for non-identical cores. These results prove that coupling lengths of MCPCF couplers are significantly shorter in μm compared to conventional multicore optical fiber couplers.

1. Introduction

The Photonic crystal fibres (PCFs) are optical fibres with air hole microstructures running along with them [1, 2]. These materials have attracted attention recently because they have unique optical properties that are not present in conventional optical fibres [2-5], such as operation in endlessly single-mode [6-8], using edge bending loss for short wavelengths [6], the fiber can provide large and small effective mode area in a single-mode region, and the anomalous group-velocity dispersion of these fibers shows two zero dispersion wavelengths in the visible and near-infrared regions [9], control dispersion management [10], low loss, high birefringence [11, 12], bio-sensing applications [13] and large mode area operation [14, 15]. There are two mechanisms for guiding light in PCFs, depending on the geometry of the fiber core; it is either a solid or hollow core [1-3, 16]. The first mechanism is known as index-guiding PCFs, which directs light by total internal refraction between the solid core and the cladding area with multiple air holes. The other mechanism uses a perfectly periodic structure appearing with a photonic bandgap at the operating wavelength to direct light into a low index hollow core region compared to the cladding region [2, 3, 13]. In this study, we use the index guiding mechanisms to guide light inside the PCF core. Through the stack and draw technique used in fabricating PCFs, it is possible to design multiple cores by compensating air holes with rods that act as coupled cores after drawing [4, 16, 17].

Recently, it was shown that a PCF design with two or more adjacent defects results in high coupling [2-4, 18-20]. This design is known as multicore photonic crystal fibres (MPCFs), which depend on the coupling behaviour between cores [5]. These MPCFs have been recently implemented in various applications for identical cores, such as couplers [18-24], power splitters [25-28], couplers based on high birefringence [29, 30], and sensors [16, 31- 32]. Non-identical cores, it can also be used in the all-optical logic operation [33], coupling [34], mode selective couplers [35], zero-differential group delay [36], high power lasers [37], polarisation splitters [38], tunable mode converter devices [39], and multiplexers and de-multiplexers [40-44]. In our study, we investigate the potential to change the coupling wavelength and improve the coupling efficiency between coupled cores depending on coupled seven-core PCF with identical and non-identical cores. The coupling properties of the proposed model, such as the coupling length and the strength of the coupling, are numerically analyzed using COMSOL MULTIPHYSICS 5.5 software and its Wave-Optics Module based on the finite element method. In this model, shorter coupling lengths of PCF- based multiplexers and demultiplexers have the potential to improve wavelength division multiplexing applications that are important for optical communication systems.

2. Theory, design methodology, simulation results and discussion

2.1. Theory for coupling behavior

We start our analysis with the assumption that the system consists of seven coupled cores of MCPCF with a hexagonal lattice. The purpose of designing the seven cores with very different structures, due to the observed change in coupling behaviour, the system of the seven coupled cores was analyzed in detail for the purpose of predicting a comprehensive system. All seven cores are identical, and each core is supposed to be a single-mode core with the propagation constant β_0, and the coupling coefficient between cores is κ. In the MCPCF, the evolution of the modal field amplitudes U_0 can be described in as in Equation (1) or (2) [36, 40, 41]:

$$i\frac{dU_0}{dz} + \beta_0 U_0 + \kappa\sum_{n=1}^{6} U_n \qquad (1)$$

We assume that the interactions are only for nearest neighbours in this system, the eigenmodes of this system take the solutions as $U_n = u_n \exp(i\beta_0 z)$ that is associated with the supermodes. The coupling coefficient κ between identical seven cores can be expressed by $\kappa_{0n} = \kappa_{n0} = \kappa$ using coupled-mode theory as [17, 40, 41] as:

$$\kappa = \sqrt{2\Delta}\,\frac{U^2}{RV^3}\,\frac{K_0(WD/R)}{K_1^2(W)} \qquad (2)$$

Δ is the normalized index difference with $\Delta = (n_{co}-n_{cl})/n_{co}$, and n_c and n_{cl} are the core and cladding refractive indices, respectively. $V=k_0 R n_{co}(2\Delta)^{1/2}$ represents a dimensionless normalized frequency number included in the eigenvalue that describes the fundamental mode LP_{01} of the core or waveguide, $UJ_1(U)/J_0(U)=WK_1(W)/K_0(W)$, where $U = R\,(k_0^2 n_{c0}^2 - \beta^2)^{1/2}, W = R\,(\beta^2 - k_0^2 n_{cl}^2)^{1/2}$, The free-space wavenumber is $k_0=2\pi/\lambda$, and R is the core radius. J_0 and J_1 represent the zeroth and first-order Bessel functions of the first kind, respectively, while K_0 and K_1 represent the zeroth and first-order modified Bessel functions of the second kind, respectively. D indicates the distance between two core centers, i.e., the core pitch. The mode propagation constant β can be defined by the eigenvalue problem as $V^2= U^2+W^2$. For the case that all cores are identical, there is no mismatch between them, and they have the same propagation constant. This leads to zero-differential group delay (ZGD) in multimode structures and thus $d\kappa/d\omega=0$. The eigenvalues of this structure satisfy the relation $d\kappa_n/d\omega= d\kappa_1/d\omega = d\kappa_2/d\omega$. This validates that the group velocities of all N supermodels are equal in case all derivatives are derived at the central frequency $\omega=\omega_0$.

This situation changes when designing a system with non-identical seven-core because coupling coefficients become different, i.e. $\kappa \neq \kappa_0 \neq \kappa_n$. Therefore, Equation (1) changes to Equation (3) if non-identical cores are designed as:

$$\frac{dU_0}{dz} + \beta_0 U_0 + \kappa_{0n} \sum_{n=1}^{6} U_n = 0 \qquad (3)$$

The coupling coefficient κ_{0n} is given by [36]:

$$\kappa_{0n} = \sqrt{2\Delta}_n \frac{U_0 U_n}{R_0 V_0} \times \frac{K_0(\frac{W_0 D_{0n}}{R_0})}{K_1(W_0) K_1(W_n)} \times \frac{\overline{W}_0 K_0(W_n) I_1(\overline{W}_0) + W_n K_1(W_n) I_0(\overline{W}_0)}{\overline{W}_0^{\,2} + U_n^2} \qquad (4)$$

The coupling coefficients κ_{0n} between the mode of the central core 0 and the nth mode core describes the change in the diameter of the central core relative to the diameters of the neighbour cores. The index difference between the refractive indices of the core $n_{co,n}$ and cladding core $n_{cl,n}$, the cladding for the nth mode core is:

$$\Delta_n = (n_{co,0} - n_{cl,n}) / n_{cl,n} \qquad (5)$$

The dimensionless number V for the central core is:

$$V_0 = k_0 R_0 n_{co,0} (2\Delta_0)^{1/2} \qquad (6)$$

$$W_0 = R_0 (\beta_0^2 - k_0^2 n_{cl,0}^2)^{1/2} \qquad (7)$$

$$U_0 = R_0 (k_0^2 n_{co,0}^2 - \beta_0^2)^{1/2} \qquad (8)$$

$$\bar{W}_0 = W_0 R_n / R_0 \qquad (9)$$

The modified Bessel functions of the first and second kind is represented by $I_n(x)$ and $K_n(x)$. The distance between the core centres for the 0th and the nth mode core is represented by D_{0n} and the core radii are R_0. It is possible to define the propagation constant β_0 from the eigenvalue problem by considering as below:

$$\beta_0 = \delta\beta_0 + \beta \qquad (10)$$

$$\beta = k_0 (n_{co}(\omega) - n_{cl}(\omega)) / 2 \qquad (11)$$

It is deleted from the derivative of the equation with respect to angular frequency, because it only depends on $\delta\beta_0$, which has only a slight difference between the propagation constants and has a relationship with the average of all the group velocities that are associated multicore PCF. To clarify the relationship between the coupling coefficient and the power flow in each core as a function of z, we consider a system that consists of two waveguides, which we label U_1, U_2. The evanescent field coupling of the waveguides can be expressed by the coupled-mode theory (CMT) equation is [41]:

$$\frac{dU_1(z)}{dz} = i\beta_1 U_1(z) + \kappa_{12} U_2(z), \frac{dU_2(z)}{dz} = i\beta_2 U_2(z) + \kappa_{21} U_1(z) \qquad (12)$$

U_1 and U_2 represent the amplitudes of these waveguides with propagation constant β_1 and β_2 along the z-direction. The coupling length κ_{ij} is described as the modal overlap between the coupled waveguides and can be expressed as:

$$\kappa_{12} = \frac{k_0^2}{2\beta} \iint_{area} (n_1^2 - n_2^2) F_1^*(x,y) F_2(x,y) dxdy \quad (13)$$

Here, n_1 and n_2 represent the refractive index profiles of the waveguide core and the background material, $F_i(x, y)$ is the modal distribution with (i=1, 2). β represents the average of the modal individual propagation constant $\beta=1/2(\beta_1+\beta_2)$. There is another explanation for the coupling between waveguides or cores of waveguides using a supermode theory that relies on specifically on hybrid modes, the two modes are describe as even (if the two modes are symmetric) or odd (if the two modes are anti-symmetric. The mode coupling strength between the cores is determined by the coupling coefficient κ and can be interpreted as the perturbations in the individual modes caused by the coupling. This gives the value for mode splitting as $\kappa = 1/2(\beta_{even} - \beta_{odd})$, where β_{even} and β_{odd} are corresponding propagation constants of even and odd modes, respectively. The constant propagation can be defined as $\beta = 2\pi n_{eff}/\lambda$ which corresponds the effective refractive index of supermodes as n_{eff} [40, 41].
The supermode refractive indexes can be calculated by numerical simulation of COMSOL MULTIPHYSICS 5.5 software based on finite element method (FEM) within the use of a Mode solver model as in the equation below [40, 41].

$$\nabla \times (\nabla u_r^{-1} \times E) - k_0^2 \varepsilon_r E = 0 \quad (14)$$

Here, the following parameters refer to k_0 , μ_r, ε_r the free space wave number, the permeability of the material and the permittivity of the material, assuming that the multicore PCF is non-magnetic $\mu_r = 1$, $\varepsilon_r = n^2$ than the equation (8) becomes as:

$$\nabla \times (\nabla \times E) - k_0^2 n^2 E = 0 \quad (15)$$

The refractive indices of the modes were extracted from the simulation so it is easy to calculate the coupling length according to the equation below:

$$L_c = \frac{\lambda}{2(n_{even} - n_{odd})} \quad (16)$$

The coupling length of the supermode is related to the coupling strength κ as $L_c = \pi/ 2\kappa$. The amount of power entering into each core as a function of z can be determined by the Poynting vector [5, 41]:

$$P_{core}(z) = \frac{1}{2} \mathrm{Re} \iint_{corearea} \vec{E}(x,y,z) \vec{H}^*(x,y,z) \cdot \hat{z} dxdy \quad (17)$$

2.2. Design methodology
The assumed structure in our study is represented by seven cores coupled PCF system as an MCPCF with identical and non-identical seven-core systems that is examined in detail to predict a large system. We use the Wave-Optics Module of COMSOL MULTIPHYSICS software which is based on finite element model for mode analysis study. We design the seven-core PCFs with five hexagonal lattices of air holes. The structural parameters of the design are pitch of **Λ**= 5.6 μm, hole diameter of d_{hole}= 4.48 μm, air-filling fraction of d/Λ = 0.8 and core separation of **2Λ**. We simulate the silica material with a core refractive index n_{core}= 1.445 that is slightly more than the cladding refractive index n_{cladd}= 1.44. Figure 1, shows the cross-section of a PCF coupler with seven identical cores when all diameters of the cores are 3.5μm. The finite element method can calculate the guided modes of the PCF coupler by directly solving Maxwell's equation according to equation (14) in order to obtain approximate values of the effective refractive indices of the modes. We evaluate the power that is exchanged between the coupled cores owe to the weak overlap of its nearby electric fields. When the light enters into one of the PCF cores as e.g. central core, the power transfers to the other cores after the propagation distance defined by the coupling length L_c, after calculating the effective refractive indices of the fundamental

mode, it becomes easy to calculate the coupling length from Equation (16) and then subsequently the coupling coefficient

2.3. Simulation results and discussion

The results from a numerical simulation based on guided mode analysis by finite element modelling show the effective indices of both the even and odd modes of the seven cores of the PCF coupler. Figure 2 shows the change in the coupling properties, such as coupling length and coupling coefficient of identical seven-core couplers dependent on the wavelength. At a wavelength of $\lambda = 1.064$ µm, we found the effective indices for even and odd modes as 1.4428 and 1.4427, respectively, which can then be used to directly calculate the coupling length of 2660 µm, and a coupling coefficient of 0.0023 µm, as shown in Figure 2 (a, b). When increasing the wavelength to $\lambda = 1.55$ µm, we found the coupling length is reduced to 968.75 µm. Because of the noticeable increasing difference in the refractive indices of both the even and odd modes to become 1.4420 and 1.4413, respectively, and the coupling coefficient is 0.0064 µm, as shown in Figure 2 (c, d). When continuing to increase the wavelength to $\lambda = 2$ µm, we notice that the coupling length gradually decreases to 714.285 µm, because of the increased difference in the refractive indices of both the even and odd modes to take the values 1.4415 and 1.4401, respectively. We also notice an increase in the coupling coefficient up to 0.0087 µm, as shown in Figure 2 (e, f). In the final case, we tried to reduce the wavelength to $\lambda = 0.5$ µm and found that the coupling does not exist any longer between the cores because there is no difference in the refractive indices of the even and odd modes, so this difference is very close to zero with the values of 1.4443 and 1.4443. Hence, the coupling length and the coupling coefficient at this wavelength are zero as well, as shown in Figure 2 (g, h).

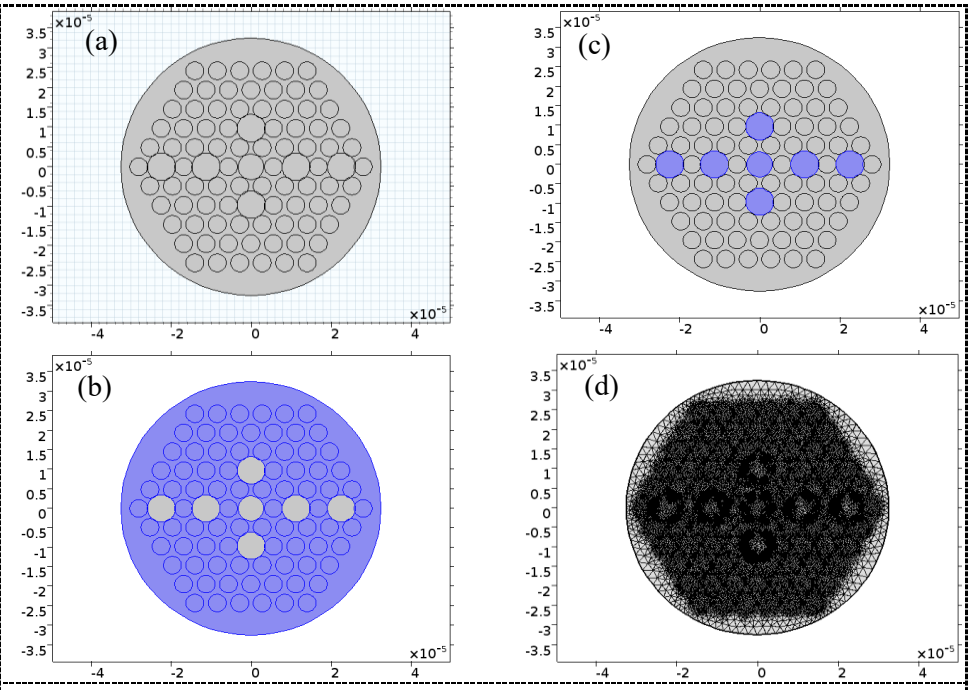

Figure 1. Cross-section of the PCF coupler consists of seven identical cores with five rings-hexagonal lattices using COMSOL MULTIPHYSICS 5.5 software: (a) geometry of the proposed structure; (b) insertion of the material for cores; (c) insertion of the material for cladding; (d) free-triangular mesh of the proposed structure.

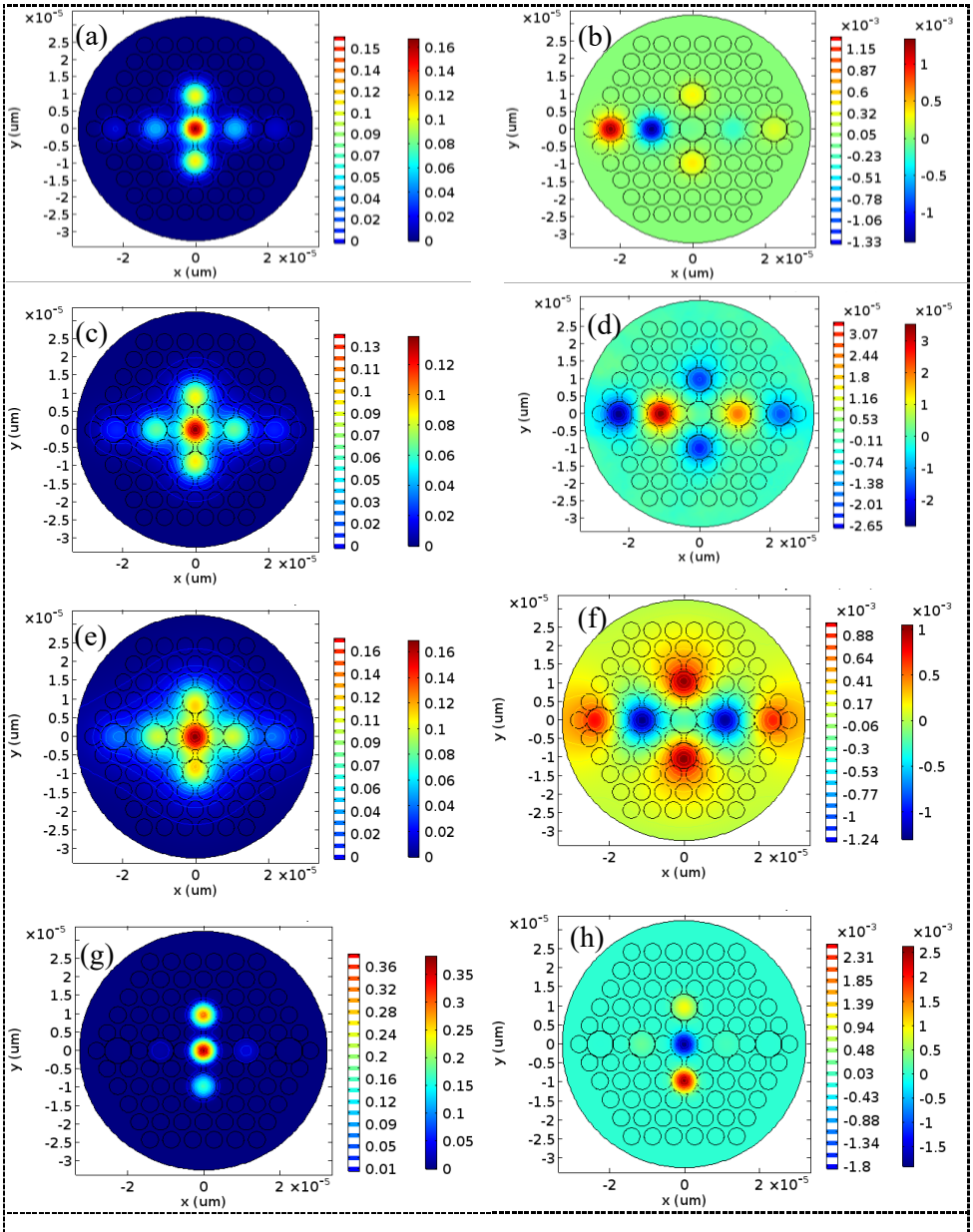

Figure 2. Surface and contour electric field (E_x) along with the x-polarized for both even and odd modes with different wavelengths (a,b) 1.064 µm; (c, d) 1.55 µm; (e, f) 2 µm; and (g, h) 0.5 µm, when all seven cores have identical diameters (d=3.5 µm).

Table 1. Represents the results of the numerical calculation for the coupling of seven cores of identical diameters as 3.5 µm at different wavelengths.

Wavelength (μm)	Even mode	Odd mode	Coupling length (μm)	Coupling coefficient $(\mu m)^{-1}$
1.064	1.4428	1.4427	5320	0.0011
1.55	1.442	1.4413	968.75	0.0064
2	1.4415	1.4401	714.285	0.0087
0.5	1.4443	1.4443	0	0

The results of Table.1 are shown in the graphic representation of Figure 3 shows the obvious difference in refractive indices between even and odd modes as a function of the wavelength is shown in Figure 3(a). We find this difference to increase with increasing wavelength for short wavelengths, but at longer wavelengths, this difference gets significantly reduced. For short wavelengths, the refractive index of the material is wavelength dependent. Due to the material dispersion, which contributes to evaluating the even and odd effective index, this dispersion becomes more prominent as for longer wavelengths. In Figure 3(b), we show that the wavelength depends on the coupling length, the coupling length decrease with increasing wavelength due to the increasing difference in refractive indices between even and odd modes. In Figure 3 (c), one can see that the coupling coefficient is strongly wavelength-dependent, and increases with increasing the wavelength.

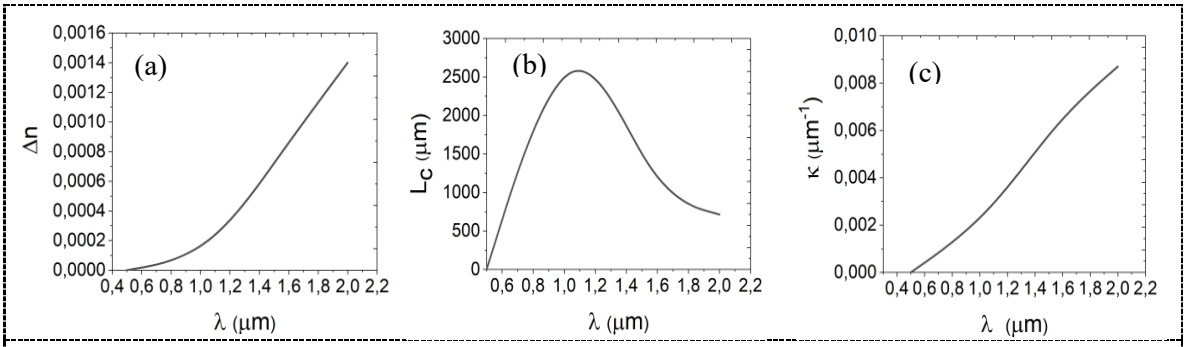

Figure 3. (a) Difference between the even and odd modes as a function of wavelength, showing that this difference increases with wavelength; (b) the coupling length gradually decreases with increasing operating wavelength; (c) the coupling coefficient is strongly dependent on the operating wavelength.

Besides, we evaluate the field distribution of the seven-core system, resulting in the fourteen fundamental modes, where each core supports two modes and it is possible to know the optical power that flows in each core when the initial input is in the central core, as shown in Figure 4 (a-d). In the case of $\lambda = 1.064\mu m$, we found the field distributions of the even mode field, such as (LP_{01}), (L P_{31}), and (LP_{11}). We find that strong coupling occurs between the central core and two adjacent cores when these two cores have propagation constants approximately equal to propagation constant of the central core as (LP_{31}). Alternatively, we found that all the power is limited to the central core as (LP_{01}). Finally, we also found from the results that strong coupling occurs between two or four adjacent cores as the power is limited in adjacent cores (high-order mode) when these cores have almost the same propagation constants, as shown in Figure 4 (a). In the case of $\lambda = 1.55$ μm, we find a weak coupling between the central core and two adjacent cores as (LP_{31}), and all the power limited to the central core as (LP_{01}), as well as, there is some strong coupling that occurs between two, four, six adjacent cores as (LP_{11}), as shown in Figure 4 (b). In the case of $\lambda = 2$ μm, we also find that there is a weak coupling between the central core and the four adjacent cores as (LP_{12}), or maybe we find strong coupling between two, three, four or maybe six adjacent cores as (LP_{11}), as shown in Figure 4 (c). In the case of $\lambda = 0.5$ μm, we find a strong and also weak coupling between the central core and only one adjacent core as (LP_{21}), or a weak coupling between the two adjacent cores, while other cores remain isolated in its place within the array of PCF without any coupling, as shown in Figure 4 (d) shows two modes of the central core represented in black and yellow, while the rest of the colours represent the modes of the cores adjacent to the central core.

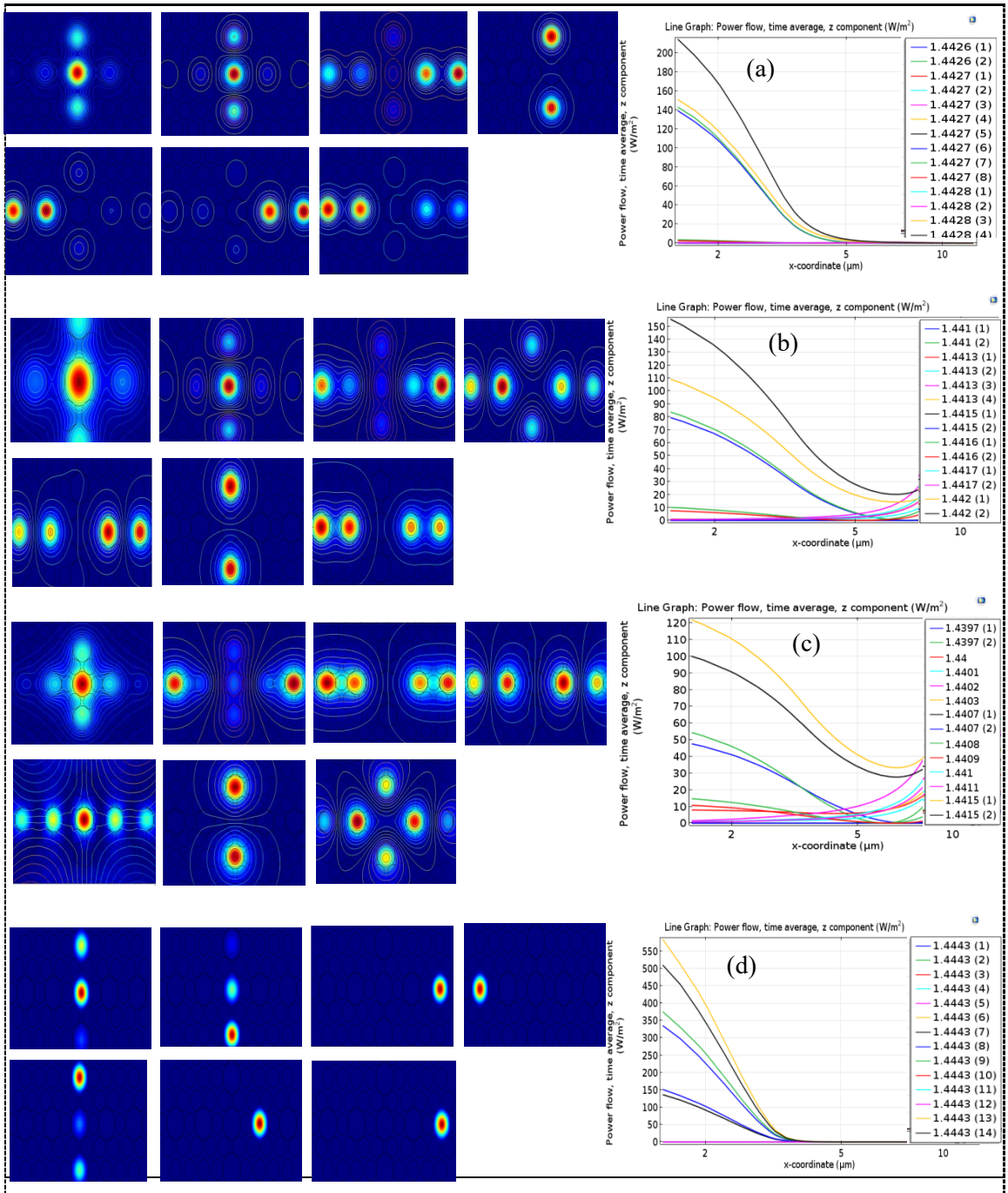

Figure 4. Surface power flow and contour distributions of the electric field norm at wavelengths of (a) 1.064 μm; (b) 1.55 μm; (c) 2 μm; (d) 0.5 μm, for a PCF coupler with a five-ring hexagonal lattice design and seven cores with identical diameters (central core = outer core = d = 3.5 μm).

Moreover, we designed anisotropy in all core diameters of the PCF coupler by changing the diameter of all cores, such as 3.2 μm, 3.5 μm, 3.47 μm, 3.49 μm, 3.52 μm, 3.54 μm, 3.56 μm. Through the results, we found that using the wavelength λ = 1.064 μm yields a coupling length that is less than the non-identical seven-core, the coupling length at this wavelength is 1773 μm and the difference in the refractive indexes of the even and odd modes are 1.4429 and 1.4426, respectively. It has a coupling

coefficient of 0.0035 μm, as shown in Figure 5 (a, b). At λ = 1.55 μm, we found that the coupling length is reduced to 1550 μm, due to the large difference in the refractive indexes between even and odd modes at 1.442 and 1.4417, respectively, and has a coupling coefficient of 0.0040 μm, as shown in Figure 5 (c, d). By increasing the wavelength to λ = 2 μm, the coupling length is reduced to 666.66 μm, because of the increased difference in the refractive indexes of the even and odd modes at 1.4415 and 1.4401, respectively, and the coupling coefficient is 0.0087 μm, as shown in Figure 5 (e, f). When decreasing the wavelength to λ = 0.5 μm, the coupling is non-existent due to the difference in the refractive indexes between the even and odd modes being zero with values 1.4443 and 1.4443, respectively. Therefore the coupling length and coupling coefficient become zero, as shown in Figure 5 (g, h).

Table 2. Represents the results of the numerical calculation of the coupling of seven cores, all of their diameters are different. The study is opposite to the first study when all seen coupled cores are identical at different wavelengths.

Wavelength (μm)	Even mode	Odd mode	Coupling length (μm)	Coupling coefficient $(\mu m)^{-1}$
1.064	1.4429	1.4426	1773	0.0035
1.55	1.442	1.4417	1550	0.0040
2	1.4415	1.4401	666.66	0.0087
0.5	1.4443	1.4443	0	0

The results of Table 2 are shown in the graphic representation of Figure 6, we observed the difference in the refractive index also increases with wavelength than for the identical state, as shown in Figure 6 (a). While in Figure 6 (b), here, we find that the coupling length decreases with increasing wavelength and we find that it has become shorter for all cases of wavelengths. In Figure 6 (c), we see that the coupling coefficient also increases with increasing wavelength and here we find that it has become slightly lower than the identical state.

Although adjustments have been made in the diameter of the central core relative to adjacent cores, we note that both the coupling efficiency and the coupling length were higher than the central core diameter remained unchanged. Figure 7 shows anisotropy in all core diameters of the PCF coupler means the non-identical core system, especially at wavelengths of λ = 1.064 μm, λ = 1.55 μm, λ = 2 μm, we found some strong coupling that occurs between the central core and four cores or two adjacent cores. In contrast, we also see some strong coupling that occurs between the central core and two adjacent cores or perhaps one of the adjacent cores in the identical cores system at wavelengths λ = 1.064 μm, λ = 1.55 μm, λ = 2 μm, and λ = 0.5 μm.

The obtained results are useful in multiplexing and demultiplexing (MUX-DEMUX) applications due to the short coupling lengths in the proposed structures. It can be seen that the coupling lengths of different wavelengths can be adjusted to design couplers of short coupler lengths compared to conventional fiber couplers. It is possible to launch the light into one core efficiently at the input and then collected from one core or more cores at the end of the PCF or maybe separate at the one core without/with little penetration into other cores depending on the wavelength of the operation.

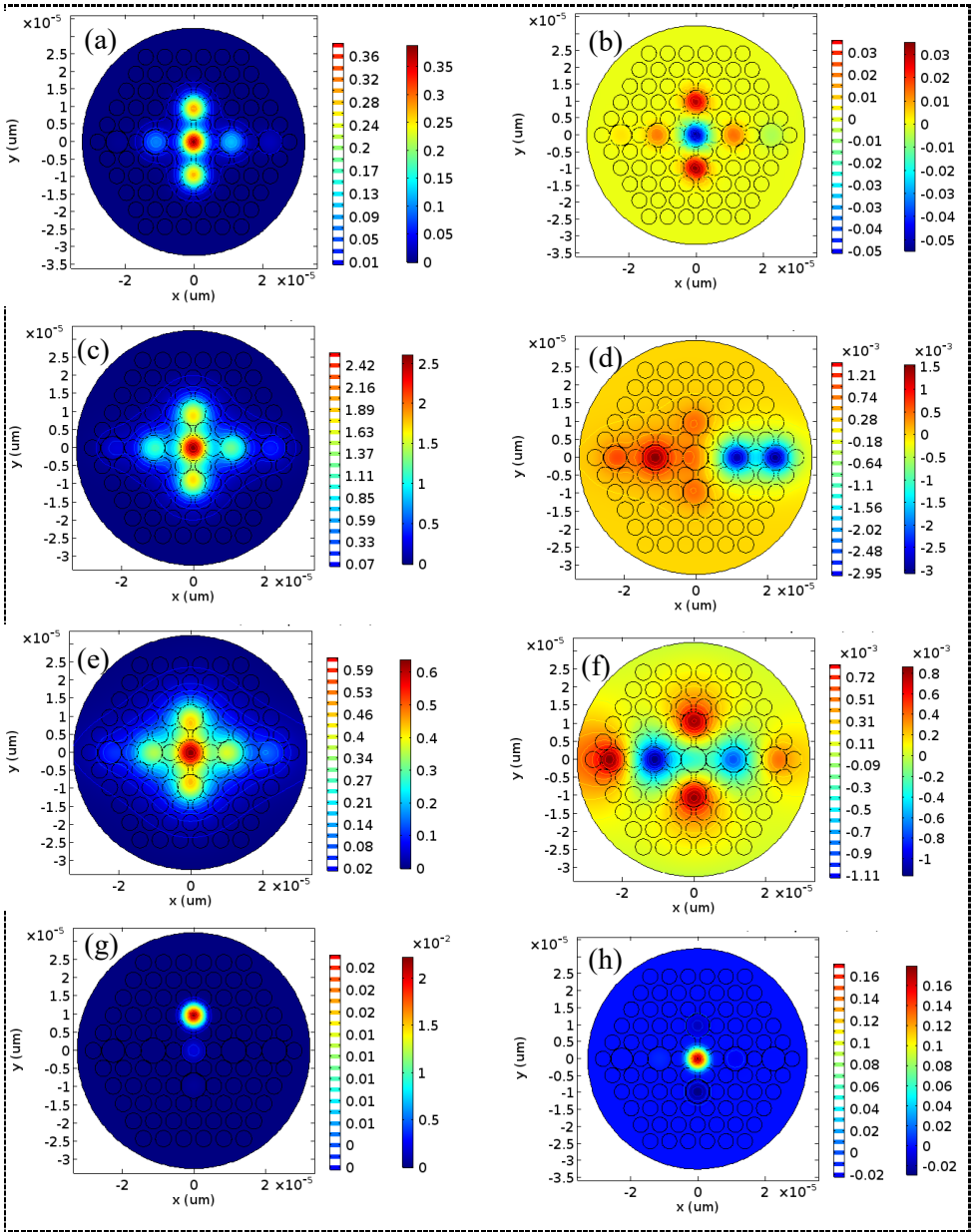

Figure 5. Surface and contour electric field (Ex) along with the x-polarized for both even and odd modes with varying wavelengths of (a) 1.064 μm; (b) 1.55 μm; (b) 2 μm; and (d) 0.5 μm. All seven cores have different diameters such as 3.5 μm, 3.2 μm, 3.47 μm, 3.49 μm, 3.52 μm, 3.54 μm and 3.56 μm.

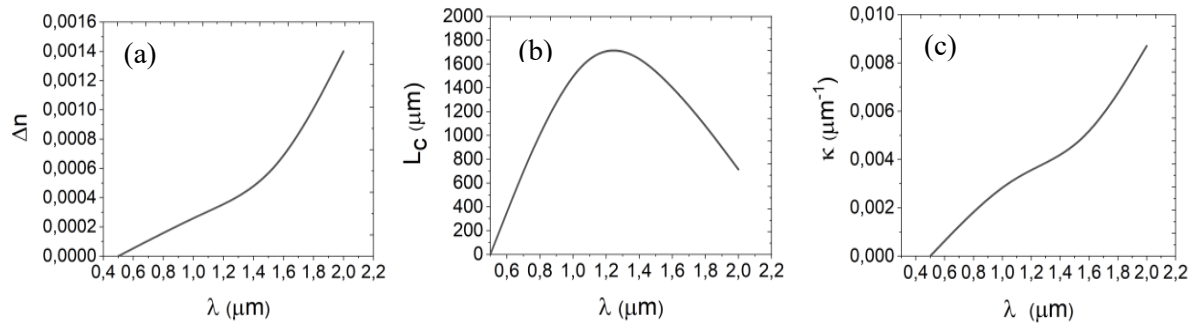

Figure 6. (a) Difference between the effective indices of the even and odd modes as a function of wavelength; (b) the coupling length gradually decreases as the operating wavelength increases; (c) the coupling coefficient is strongly dependent on the operating wavelength. All seven cores have different diameters 3.5 μm, 3.2 μm, 3.47 μm, 3.49 μm, 3.52 μm, 3.54 μm and 3.56 μm.

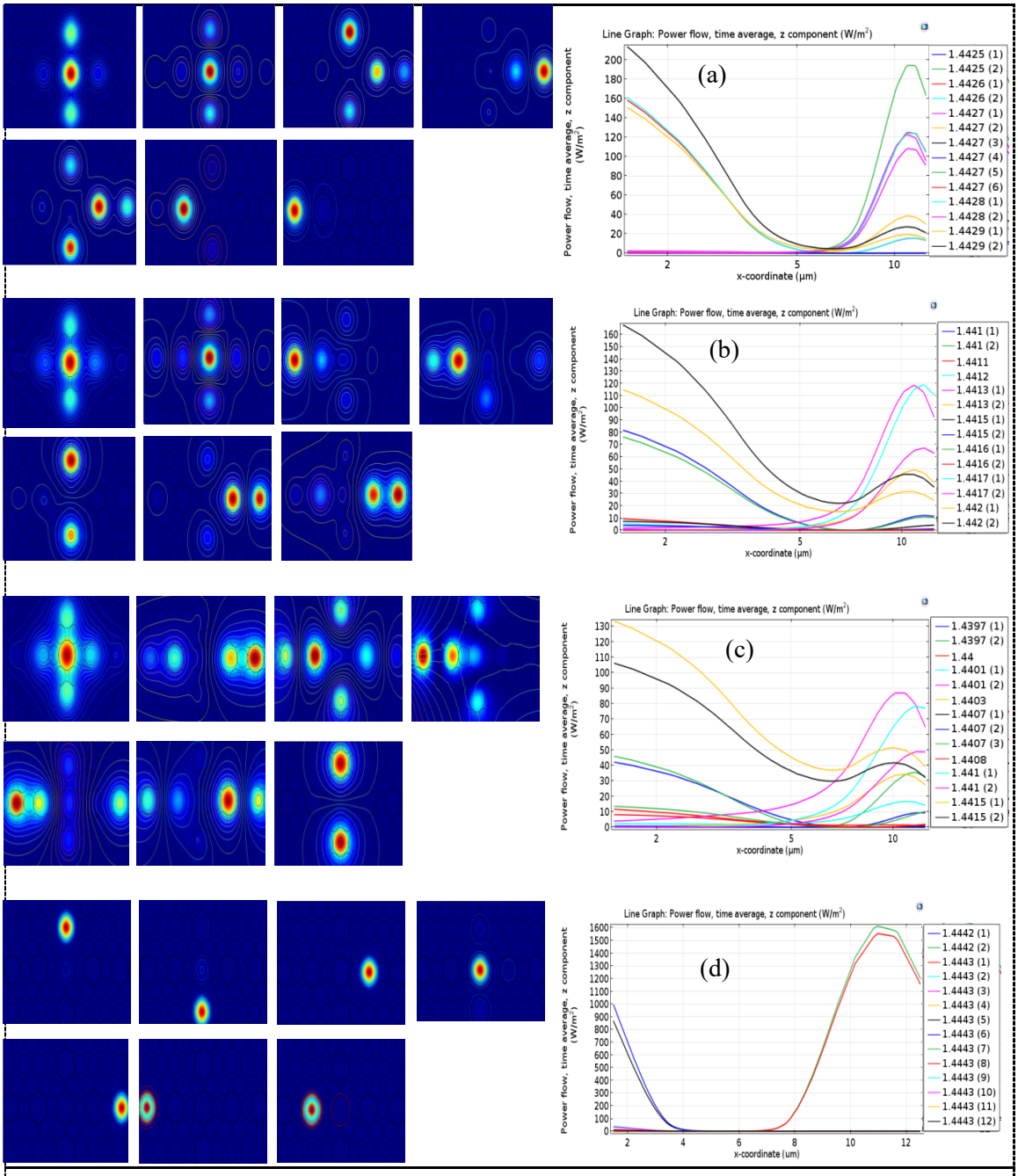

Figure 7. Surface power flow and contour distributions of the electric field norm at wavelengths of (a) 1.064 µm; (b) 1.55 µm; (c) 2 µm; (d) 0.5 µm, for a PCF coupler with a five-ring hexagonal lattice design and seven cores with different diameters (3.5 µm, 3.2 µm, 3.47 µm, 3.49 µm, 3.52 µm, 3.54 µm and 3.56 µm).

Our findings for the first time using four different wavelengths as 1.064 µm, 1.55 µm, 2 µm, 0.5 µm. Our results in this study were much better than previous studies [5, 22, 24], in terms of strong coupling and according to the engineering design of the new structure of the system that was designed by us. In previous studies [5, 22, 24], which used one, two or maybe three wavelengths, as we made a coupling between the fiber cores in a different way by changing the small diameters of the central core of the fiber with respect to the outside cores. In addition, we investigated the effect of a change in wavelength on the coupling efficiency, i.e. in other words

we study the wavelength as a function of coupling efficiency when we create anisotropy in the diameters of all cores of the photonic crystal fibers. Therefore, we also designed in this study a unique and new system for the first time and used four wavelengths that gave the best results in terms of the coupling between seven cores completely dissimilar in all their small diameters if compared to the results in [36]. Because a small anisotropy is used in all the diameters of the cores, it is sufficient to cause uncoupling between the seven cores and suppress the coupling between them, and as a result the patterns for these cores become uncoupled and remain isolated as they can within the region in the fiber geometry array. By using four wavelengths, we broke this barrier of non-coupling, and we were able to obtain good coupling between the cores by increasing the wavelength even though all cores are completely different in their diameters our results are useful in applications such as couplers, multipliers and de-multipliers

3. Conclusions

A theoretical study was used to design a new type of multi-core optical crystal fiber that depends on predicting the behaviour of strong coupling between the seven coupled cores, COMSOL MULTIPHYSICS Software based mainly on the finite element method was used. Small random changes in the diameters of these seven cores result in a variation in the photonic crystal fiber structure, and thus a mismatch in the refractive index of the fundamental modes of these individual cores. It is clear from the results that despite the presence of this random variation in the diameters of all cores, which would weaken or suppress the coupling between cores, there is a strong mode coupling between the central core and two or four adjacent cores, and the reason is that the modes of those cores have propagation constants almost identical. That is, their modes have zero phase mismatches. As a result, the coupling efficiency between the cores becomes better and the coupling length is lower than that of the identical cores. In addition, the coupling efficiency between the coupled cores is a function of the wavelength used. This means, the coupling efficiency was stronger for wavelength $\lambda = 1.064$ μm, followed by $\lambda = 1.55$ μm and $\lambda = 2$ μm, while suppressed at a wavelength of $\lambda = 0.5$ μm, where the cores remain isolated in their place without coupling, or they stay in place with little penetration into other cores. From all this we conclude, that it is possible to design multi-core photonic crystal fiber couplers of varying diameters that have shorter coupling lengths in micrometers compared to optical fiber couplers whose coupling lengths are designed in millimeters. These devices can be used in applications such as MUX-DEMUX or can be used as a power coupler in an application, such as wavelength division WDM systems.

Acknowledgments

This work was partially supported by the Republic of Iraq Ministry of High Education& Scientific Research scholarship (MoHESR Grant No. 16408). And also author acknowledges the University of Muenster-department of physics, Germany to support.

References

[1] Wei J, Jian J, Hoi L, Yeuk L, Ailing Z 2013, *J.Optoelectron.* **6** 3-24.
[2] Saitoh K, Sato Y, Koshiba M 2003 *J. Opt. Express* **24** 3188-3195.
[3] Khan K, Wu T 2008, *J. ACES* **3** 215.
[4] Huimei H, Wang L 2013, *J. Optik* **124** 5941-5944.
[5] Reichenbach K L, Xu C 2005, *J. Opt. Express* **25** 10336-10348.
[6] Birks T A, Knight J C 1997, *J. Opt. Lett*. **22** 961-963.
[7] Saitoh K, Tsuchida M, Koshiba M, Mortensen N A 2005, *J. Opt. Express* **13** 10833-10839.
[8] Poli F, Selleri A 2007 *Photonic Crystal Fibres: Properties and Applications*, 1st edn., (Springer).
[9] Gander M J, McBride R, Jones J D C, Mogilevtsev D, Birks T A, Knight J C, Russell P S J 1999, *J. Electron. Lett.* **35** 63-64.
[10] Saitoh K, Koshiba M, Hasegawa T, Sasaoka E 2003 *J. Opt. Express* **11** 843-852.
[11] Reyes E, Suga-Restrepo J, Jime´nez-Durango C, Montoya-Cardona J, Omez-Cardona N 2018, *J. IEEE Photon*. **10** 5900413.
[12] Chen D, Shen I 2000, *J.* Opt. Lett. **25** 1325-1327.
[13] Ahmad A K and Khalifa Z 2020 *AIP Proc. Int. Conf. on Material Engineering & Science (IConMEAS)* in (Baghdad-Iraq) **2213** 020131.

[14] Knight J C, Birks T A, Cregan R, Russell P S J, De Sandro J P 1998 *J. Electron. Lett.* **34** 1347-1348.
[15] Belardi W, Bouwmans G, Provino L, Pureur V, Douay M 2006 *Proc. Int. Conf. on Optical Fibre Communication Conference (OFC),* Optical Society of America, p. OFC3.
[16] Moutusi D, Tarun K G, Vinod K S 2019, *J.* Sensors **19** p. 464.
[17] Yu X, Liu M, Chung Y, Yan M, Shum P 2006, *J. Opt. Commun.* **260** 164-169.
[18] Yuan C, Shi J 2010, *J.* Opt. Commun. **283** 2686-2689.
[19] Rohini K, Raja A, Sunda D 2015, *International Journal of Engineering, Management & Sciences (IJARTET*) **II**, 2394 –3785.
[20] Mohammed M 2019 *Proc. Int. Conf. on Computational Methods in Engineering Science (CMES 2019)* in (Kazimierz Dolny- Poland) **ISBN: 978-83-7947-386-1** p.74-87.
[21] Mohammed D, Mohammed C 2014, *J. Electrical & electronics engineering* **7** 9-12.
[22] Reichenbach K L, Xu C 2007, *J.Opt. Express* **15** 2151-2156.
[23] Ren W, Tan Z, Ren G 2015, *J. IEEE Photon. Soc.* **7** 7100311.
[24] Wang J., Nadkami S. 2014, *J. Opt. Express* **22** 8908-8918.
[25] Malka D, Peled A 2017*, J. Appl. Surf. Sci.* **417** 34-39.
[26] Xu Q, Luo W, Li K , Copner N, Lin S 2019, *J. Crystals **9*** 103.
[27] Eyal C, Zeev Z, Eyal C 2017, *J. Appl. Sci. 7* 695.
[28] Shu X, Zhenpeng W, Qianhui D, Kai T, Xiaoxo R, Mingxin Y 2019 *Proc. Int. Conf. on Advanced Optical Manufacturing and Technologies Conference: Optoelectronic Materials and Devices for Sensing and Imaging* **108430**.
[29] Reyes-Vera E, Suga-Restrepo J, Jime´nez-Durango C, Montoya-Cardona J, Gomez-Cardona N 2018, *J. IEEE Photon.* **10** 5900413.
[30] Hanna I, Maciej A 2019, *J. Fibres* **7** 109.
[31] Wang J, Zhang Z, Li S, Wang S 2019*, J. Modern Phys. Lett.* **B 33** 1950380.
[32] Zhilong O, Yongqin Y, Peiguang Y, Jishun W, Quandong H, Xue Ch, Chenlin D, Huifeng W 2013, *J .Opt. Express* **21** 23812 23821.
[33] Uthayakumar T, Raja R V J, Porsezian K, Grelu P 2015, *J . Opt. Soc. Am.* **32** 1920-1928.
[34] Szostklewicz L, Napierala M, Ziolowicz A, Pytel A, Tenderenda T, Nasilowski T, 2016, *J .Opt. Lett.* **41** 3759.
[35] Reyes-Vera E, Úsuga J, Gómez-Cardona N, Varón M 2016, *Proc. Int. Conf. on Latin America Optics and Photonics* (OSA).
[36] Parto M, Amen M, M-ALI M, Amezcua R, LI G, Christodoulides D N 2016, *J . Opt. Lett.* **41** 1917-1920.
[37] Chen Y, Yang D, Zhang B 2018, *Proc. Int. Conf. on Micro-Structured and Specialty Optical Fibres,* SPIE **10681**106810X.
[38] Younis B, Heikal A, Mohamed F, Obayya S 2018, *J . Opt. Soc. Am.* **B 35** 1020-1029.
[39] Andres J, Dario N, Gonzalez E P T, Reyes E, 2020, *J . Photonics* **7** p. 3.
[40] Miami M and Ahmad K A 2020, *Rafidain Journal of Science (RJS)*, **29** 16-27.
[41] Miami M and Ahmad K A 2020, *AL-Nahrain Journal of Science (ANJS)* **23** 49-60.
[42] Mohammed M and Ahmad K A 2021. *J. Phys.: Conf. Ser.* **1736** 012037.
[43] Miami M 2021 *Proc. Int. Conf. on Metamaterials, Photonic Crystals and Plasmonic* (*META 2021)* in (Warsaw – Poland), **ISSN 2429-1390** 20-23.
[44] Mohammed M and Ahmad K A 2021. *J. Phys.: Conf. Ser.* **2130** 012035.